

# Asymmetric Ion Transport through Ion-Channel-Mimetic Solid-State Nanopores

WEI GUO, YE TIAN, AND LEI JIANG\*

*Beijing National Laboratory for Molecular Sciences (BNLMS), Key Laboratory of Organic Solids, Institute of Chemistry, Chinese Academy of Sciences, Beijing 100190, People's Republic of China*

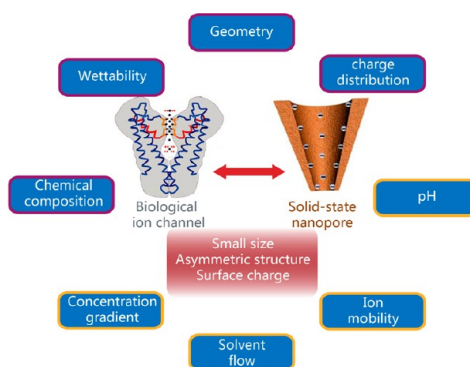
RECEIVED ON JANUARY 30, 2013

## CONSPECTUS

Both scientists and engineers are interested in the design and fabrication of synthetic nanofluidic architectures that mimic the gating functions of biological ion channels. The effort to build such structures requires interdisciplinary efforts at the intersection of chemistry, materials science, and nanotechnology. Biological ion channels and synthetic nanofluidic devices have some structural and chemical similarities, and therefore, they share some common features in regulating the traverse ionic flow. In the past decade, researchers have identified two asymmetric ion transport phenomena in synthetic nanofluidic structures, the rectified ionic current and the net diffusion current. The rectified ionic current is a diode-like current–voltage response that occurs when switching the voltage bias. This phenomenon indicates a preferential direction of transport in the nanofluidic system. The net diffusion current occurs as a direct product of charge selectivity and is generated from the asymmetric diffusion through charged nanofluidic channels. These new ion transport phenomena and the elaborate structures that occur in biology have inspired us to build functional nanofluidic devices for both fundamental research and practical applications.

In this Account, we review our recent progress in the design and fabrication of biomimetic solid-state nanofluidic devices with asymmetric ion transport behavior. We demonstrate the origin of the rectified ionic current and the net diffusion current. We also identify several influential factors and discuss how to build these asymmetric features into nanofluidic systems by controlling (1) nanopore geometry, (2) surface charge distribution, (3) chemical composition, (4) channel wall wettability, (5) environmental pH, (6) electrolyte concentration gradient, and (7) ion mobility. In the case of the first four features, we build these asymmetric features directly into the nanofluidic structures. With the final three, we construct different environmental conditions in the electrolyte solutions on either side of the nanochannel.

The novel and well-controlled nanofluidic phenomena have become the foundation for many promising applications, and we have highlighted several representative examples. Inspired by the electrogenic cell of the electric eel, we have demonstrated a proof-of-concept nanofluidic reverse electro dialysis system (NREDS) that converts salinity gradient energy into electricity by means of net diffusion current. We have also constructed chirality analysis systems into nanofluidic architectures and monitored these sensing events as the change in the degree of ionic current rectification. Moreover, we have developed a biohybrid nanosystem, in which we reconstituted the FOF1-ATPase on a liposome-coated, solid-state nanoporous membrane. By applying a transmembrane proton concentration gradient, the biohybrid nanodevice can synthesize ATP *in vitro*. These findings have improved our understanding of the asymmetric ion transport phenomena in synthetic nanofluidic systems and offer innovative insights into the design of functional nanofluidic devices.



## 1. Introduction

Design and fabrication of synthetic nanofluidic architectures that mimic the gating functions of biological ion channels have elicited considerable interest to both the scientific and engineering communities,<sup>1</sup> and represent the

forefront of the interdisciplinary fields of chemistry, materials science, and nanotechnology.<sup>2</sup> Biological ion channels and synthetic nanopores exhibit some chemical and structural resemblance, such as small size, asymmetric structure, and surface-charged channel walls (Figure 1A). Therefore,

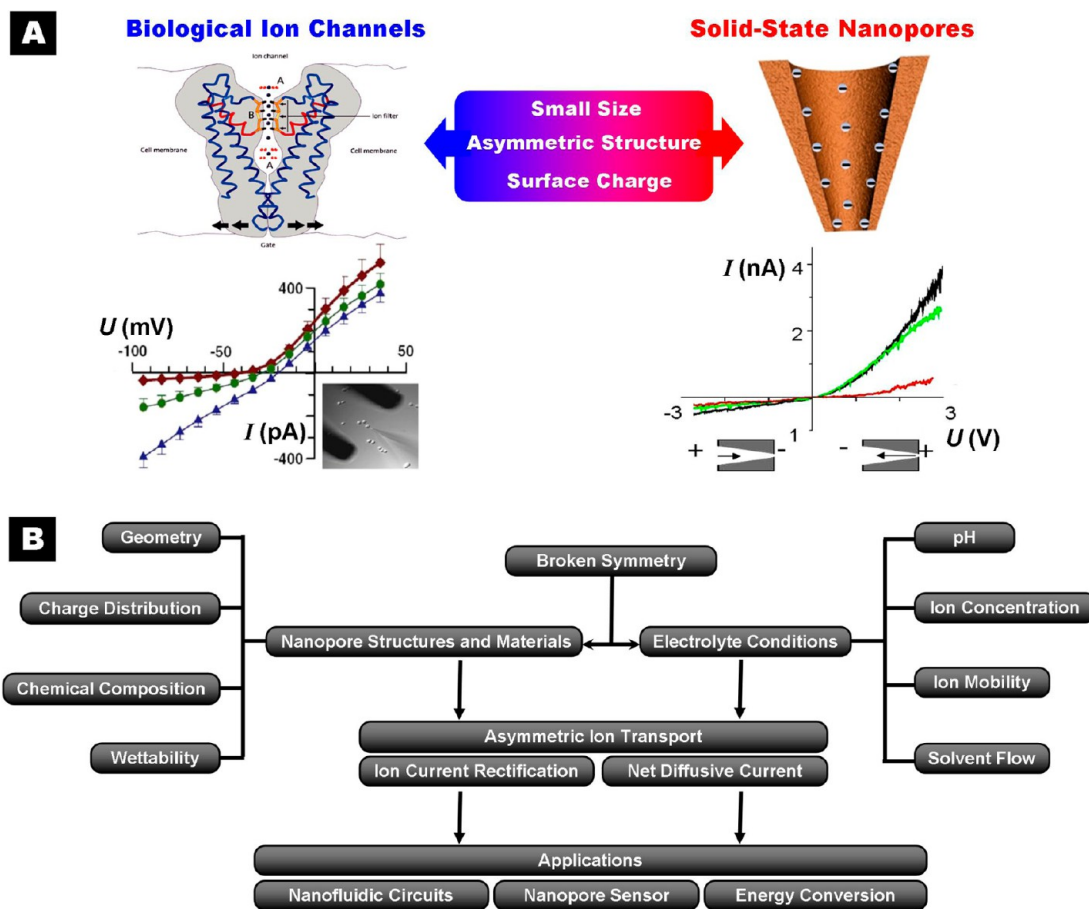


**FIGURE 1.** Designing principles of ion-channel-mimetic solid-state nanopores. (A) Biological ion channels and synthetic nanopores share some common features, such as small size, asymmetric structure, and bearing surface charge. Consequently, they show similar capabilities in regulating traverse ion transportation. (B) The asymmetric ion transport properties, including ion current rectification and net diffusion current, result from the broken symmetry, either in the nanofluidic structures or in the solution environment. The asymmetric ion transport features will eventually find applications in constructing nanofluidic circuits, nanopore-based sensing devices, bioinspired energy conversion systems, etc.

they share some common features in regulating the traverse ionic transport, particularly, in an asymmetric way. For example, they rectify the transmembrane ionic current.<sup>3</sup> The concept and design principles of our research toward bioinspired smart nanofluidic systems originate from the biological structures and new ion transport phenomena.

In the past decade, two asymmetric ion transport phenomena have been identified in synthetic nanofluidic structures, the rectified ionic current and the net diffusion current.<sup>4</sup> The rectified ionic current is observed as a diode-like current–voltage response when switching the voltage bias and indicates a preferential transport direction in the nanofluidic channel.<sup>5</sup> The net diffusion current is generated from the asymmetric ion diffusion through charged nanochannels,<sup>6</sup> a direct product of charge selectivity. These asymmetric ion transport features result from the symmetry broken in the nanofluidic system, either in the structure or in the fluidic environment.

In this Account, we review our recent progress on design and fabrication of biomimetic solid-state nanofluidic devices with asymmetric ion transport behavior (Figure 1B). We demonstrate the origin of the ionic current rectification (ICR) and the net diffusion current. We also identify several influential factors and discuss how to build these asymmetric factors into nanofluidic systems by controlling (1) nanopore geometry, (2) surface charge distribution, (3) chemical composition, (4) wettability on the channel wall, (5) environmental pH, (6) electrolyte concentration gradient, and (7) ion mobility. These important factors can be divided into two categories: factors 1–4 are asymmetric factors that can be built into the nanofluidic structures, while factors 5–7 are asymmetric factors that can be controlled in the electrolyte solutions. These new fluidic phenomena become the foundation for many promising applications. Herein, we highlight several representative examples, including bioinspired energy conversion systems, nanopore-based chirality sensing devices, and biohybrid nanodevices for *in vitro* biosynthesis.

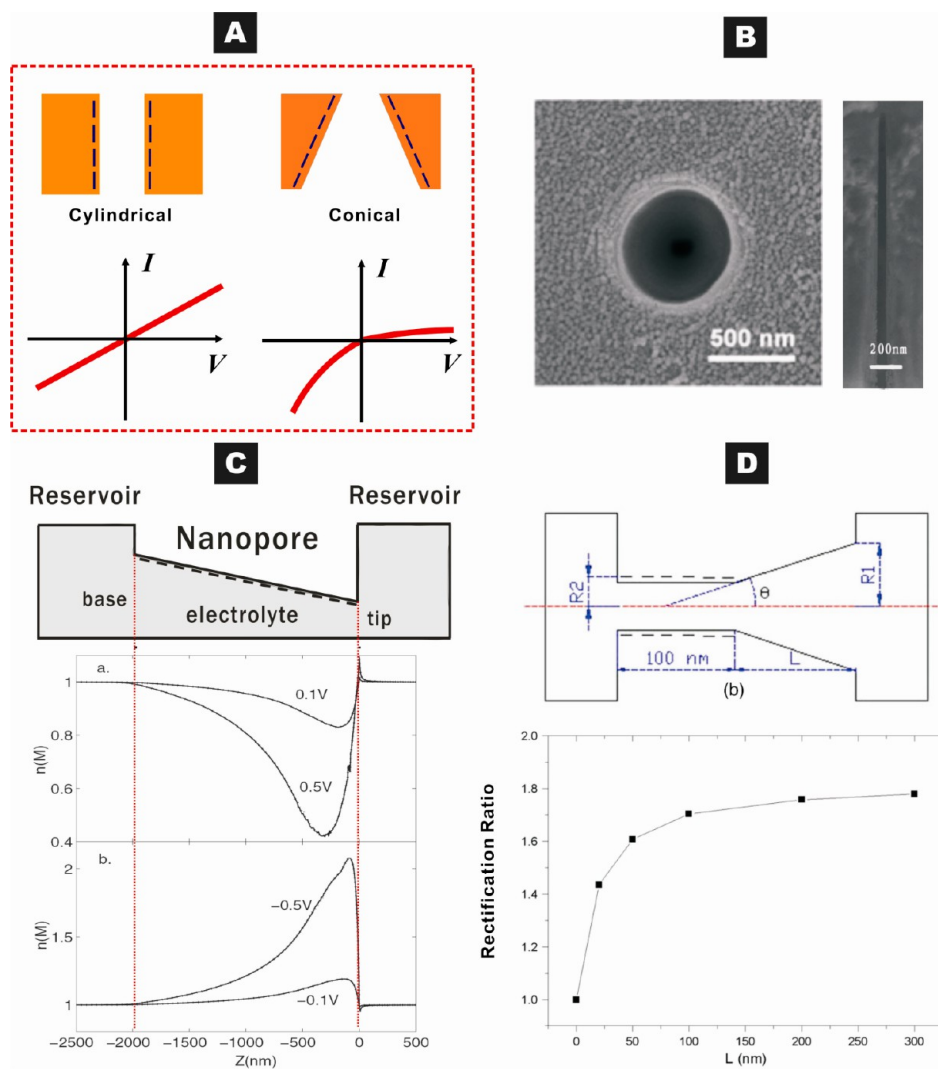


**FIGURE 2.** Ionic current rectification in geometrically asymmetric nanopores. (A) Linear  $I$ – $V$  behavior is found in cylindrical nanopores, even if they bear surface charge, but diode-like  $I$ – $V$  behavior is found in charged conical nanopores. (B) SEM image of a single conical nanopore from the base side and the cross-sectional view. (C) Theoretical results show that in a conical nanopore, the asymmetric  $I$ – $V$  behavior is due to the ion concentration enrichment and depletion effects under opposite electrical bias. (D) The asymmetric geometry is important to ICR effect. The rectification ratio increases with the length of the asymmetric part, even if it is uncharged.

It is worth mentioning that, besides ionic species, synthetic or biopolymers can translocate through the nanopores, which is well-established as a single-molecule sensing platform. Detailed information is summarized in some recent reviews.<sup>7,8</sup> Other biomimetic ion-channel systems, including self-organized macrocyclic architectures in bilayer membranes<sup>9–11</sup> and aligned carbon nanotube membranes,<sup>12</sup> have also been described in previous literature by other groups and will not be discussed in this Account.

## 2. Asymmetric Ion Transport Resulting from Nanopore Structures and Materials

Biological ion channels that regulate the ionic flow into and out of the cell membranes are of great importance to many

physiological functions. The components of the protein channels are always asymmetrically distributed across the cell membrane.<sup>13</sup> Inspired by these features, synthetic nanofluidic architectures possessing structural or chemical asymmetries show great potential in constructing biomimetic nanodevices.<sup>14</sup>

**2.1. Nanopore Geometry and Surface Charge Distribution.** Since the discovery of voltage-dependent ICR in single conical nanopores,<sup>15</sup> a full understanding of these phenomena has attracted broad interest (Figure 2A,B). In principle, a surface-charged nanopore is expected to display rectified ion transport if one end of the nanopore is geometrically larger than the other, and the diameter of the small end is comparable to the Debye screening length.<sup>5</sup> Through a

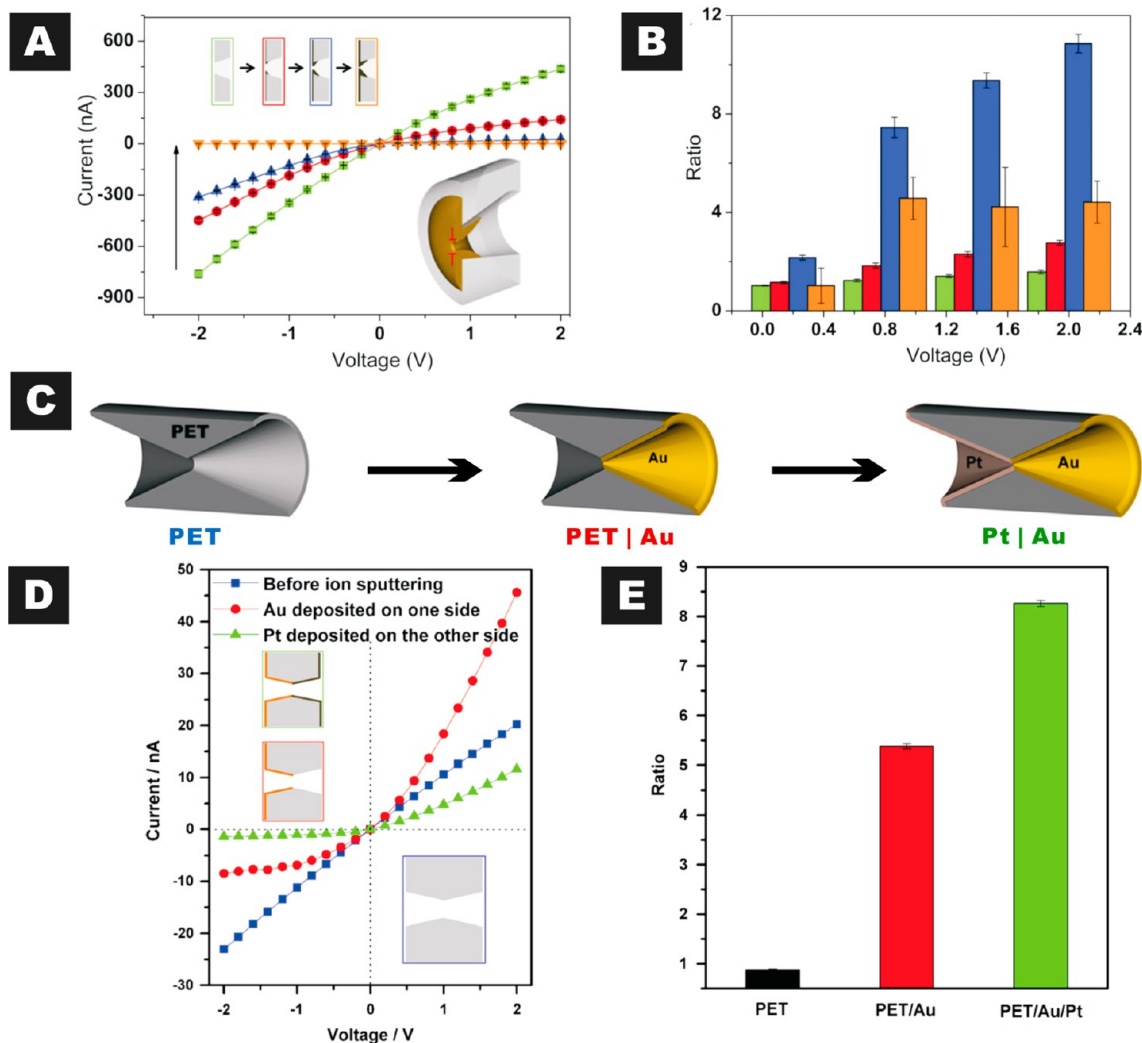


**FIGURE 3.** Ionic current rectification in metal-coated nanopores. (A, B) Single conical nanopores in polymer membrane were coated with platinum on the tip side by ion sputtering. The coated platinum layer gradually blocks the ion transport through the nanopores, but results in an enhanced rectification ratio before the nanopores are fully closed. (C–E) Hourglass-shaped nanopores were metalized with gold and platinum on separate ends. The presence of metal heterogeneous structures greatly enhances the ionic rectification.

model calculation based on Poisson–Nernst–Planck (PNP) equations, we show that the ICR is attributed to the ion-concentration enrichment at negative bias and ion-concentration depletion at positive bias (Figure 2C).<sup>16</sup> Compared with the cylindrical nanopores, the concentration enrichment and depletion in conical nanopores are deformed due to the specific geometry. Upon continual decrease of the cone angle of the nanopore,<sup>17</sup> the enrichment and depletion regions shift toward the base end, which is consistent with the calculation<sup>18</sup> and experimental<sup>19</sup> results in cylindrical nanopores.

Another important geometric parameter is the length of nanopore.<sup>20</sup> Based on the theoretical model, we propose that a relatively long length of the nanopore is indispensable for a notable rectification effect.<sup>16</sup> It is the cooperative

interaction of the small dimension on the tip side and the sufficiently long nanopore wall that contributes to the prominent enrichment and depletion of ion concentration inside the nanopore. In addition, for a conical nanopore, the ion transport property is governed by the tip region whose dimension is comparable to the electric double layer (EDL). Therefore, it is reasonable to just take a relatively short length near the tip end in the model calculation to reduce the scale of computation.

The asymmetric geometry is of significant importance to the ICR, even if the asymmetric part is uncharged (Figure 2D).<sup>21</sup> For a partially charged cylindrical nanopore ( $R_1 = R_2$ ), strong rectification effect is observed. With an enlarged  $R_1$ , the concentration enrichment and depletion become weaker inside the nanopores, leading to a decreasing

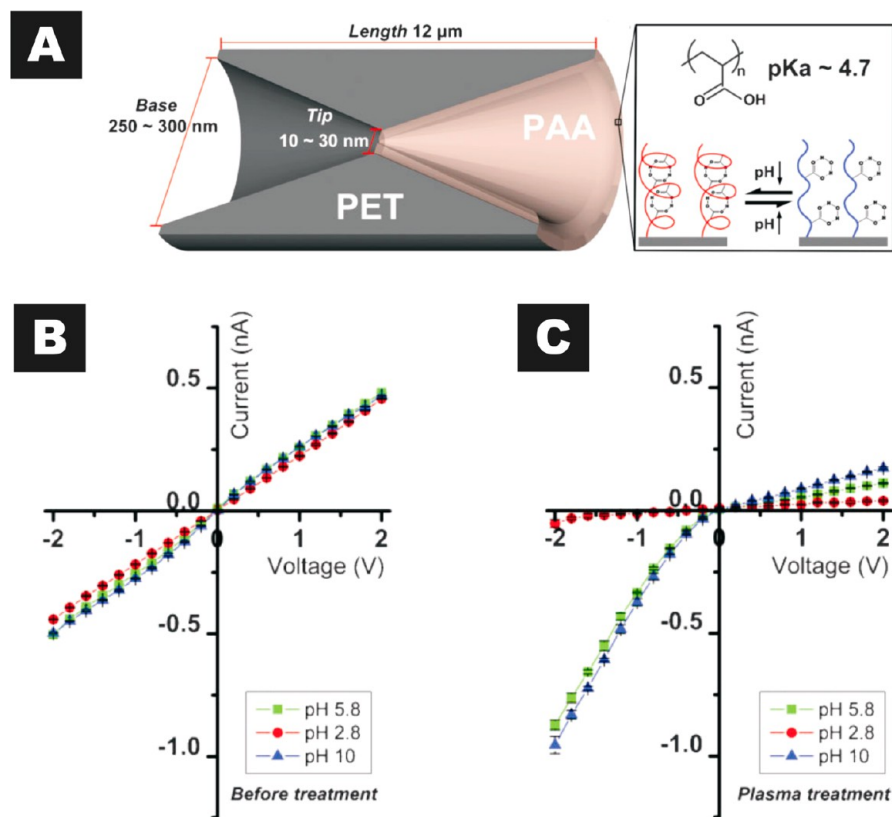


**FIGURE 4.** Ionic current rectification in polymer modified nanopores. (A) Hourglass-shaped nanopores are chemically modified with poly(acrylic acid) (PAA) on only one side. (B, C) In contrast to the unmodified nanopores showing non-pH-responsive and linear current–voltage properties, the asymmetrically modified nanopores show pH-tunable ionic current rectification.

rectification ratio. Prolonging the length of the uncharged part enhances the asymmetry in ionic conductance under the two opposite voltage bias.

**2.2. Asymmetrically Distributed Metal Coatings.** Metal nanotubule membranes show permselective ion transport properties.<sup>22</sup> Excess charge density is present on the inner surface of the metal nanotubules that dominates the trans-membrane transportation of mass and charged species. Thus, metal-coated conical nanopores rectify ionic current,<sup>23</sup> and the degree of rectification can be controlled through further chemical modification.<sup>24</sup> We fabricated a platinum-coated single nanopore by an ion sputtering technique (Figure 3A,B).<sup>25</sup> Very clear ICR is observed after platinum coating, either on the tip side or on the base side. The degree of rectification can be greatly enhanced before the nanopores are completely blocked by the sputtered metal layer. The local platinum coating brings both chemical and structural asymmetry to the nanopores that eventually results in amplified rectification.

Another method to endow nanopores with asymmetric ion conductivity is to decorate them with different kinds of metal. For example, we metalized the hourglass-shaped

single nanopores with gold and platinum on separate ends (Figure 3C).<sup>26</sup> Before metal deposition, the nanopore shows a linear current–voltage curve (Figure 3D,E). Once gold is deposited on only one side of the nanopore, the current–voltage curve shows clear rectification. As the gold layer is deposited on both the two ends, the ion transport property returns to linear. The deposited gold layers merely reduce the effective cross section of the nanopore. But, if we deposit gold and platinum on separate parts of the nanopore, it further rectifies the ionic current, owing to the heterogeneous metallic composition along the pore wall.

**2.3. Asymmetric Chemical Modification with Organic Molecules.** Besides inorganic materials,<sup>27</sup> organic molecules are also highly suitable for chemical modification of nanofluidic devices.<sup>28–30</sup> They offer profuse functional groups on the polymeric chain; therefore, electrostatic interaction, steric hindrance, and hydrophobic interaction can be introduced into the nanofluidic system.<sup>4</sup> Recently, we developed several smart nanofluidic systems with ionic gating and ionic rectifying properties by modifying polymers.<sup>31–35</sup> However, in these nanosystems, the modification covers the whole interior surface of the nanochannels.

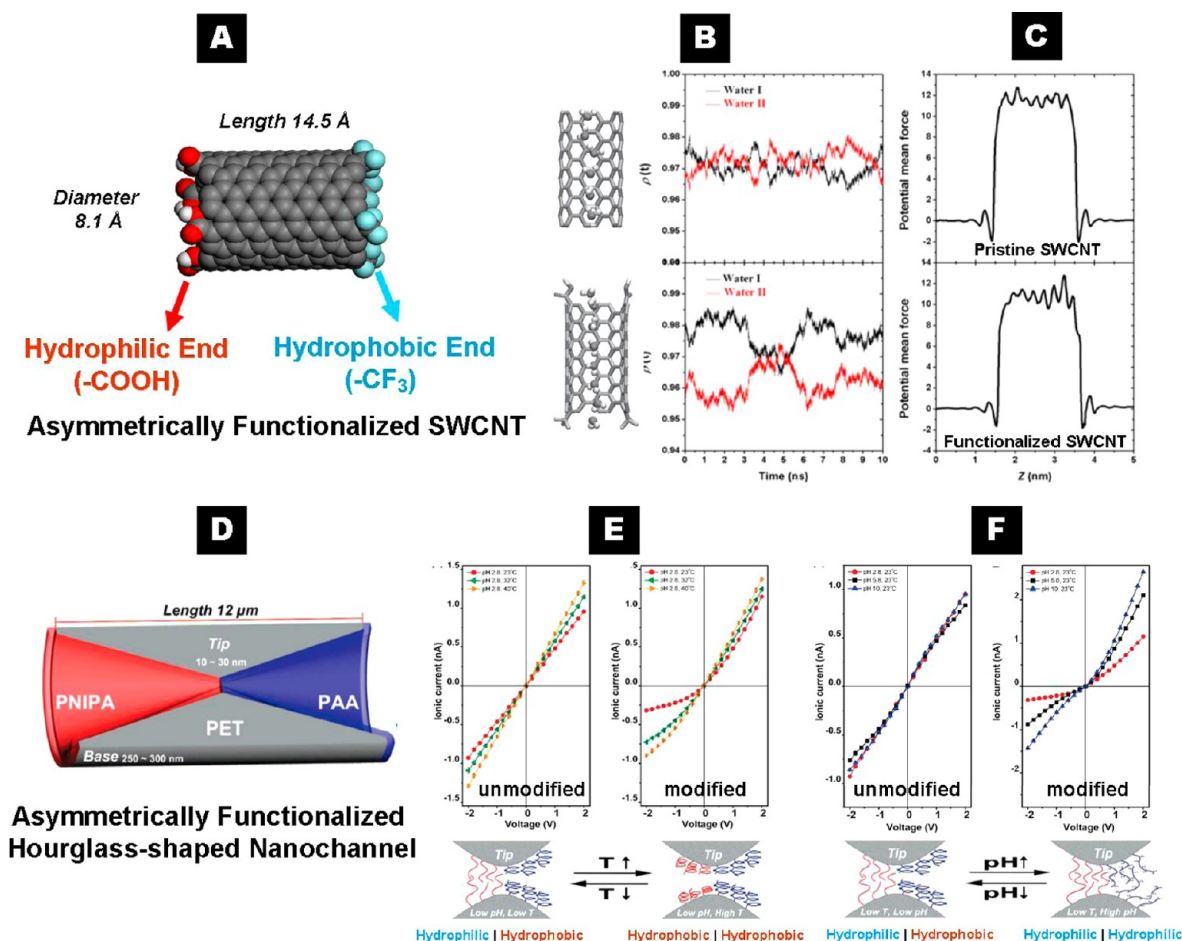


**FIGURE 5.** Water and ion transport driven by wettability gradient. (A) By MD simulation, a single-wall carbon nanotube (SWCNT) is modified with hydrophilic groups ( $-\text{COOH}$ ) and hydrophobic groups ( $-\text{CF}_3$ ) on separate ends. (B) The water density ( $\rho(t)$ ) for water I and II exhibits frequent overlap in pristine nanotubes, but in the modified nanotube, reduced water density is found on the hydrophobic side (water II). (C) The energy barrier at the hydrophilic end is slightly higher than that at the hydrophobic end. (D) Experimentally, we modified hourglass-shaped nanopores with PNIPAm and PAA on separate sides. (E, F) Asymmetric chemical composition inside the nanopore leads to rectified ionic current. Moreover, the presence of a wettability difference between the two sides enhances the degree of rectification.

By employing a plasma modification approach, we demonstrate an asymmetric modification strategy that precisely functionalizes a specific area of the nanopore with polymer brushes.<sup>36</sup> An hourglass-shaped single-nanopore is treated on only one side by plasma-induced polymerization in vapor phase of acrylic acid monomers (Figure 4A). pH-responsive poly(acrylic acid) ( $\text{pK}_a \approx 4.7$ ) is formed on the right half of the nanopore. The conformation and wettability of the polymer brushes transits from coiled/hydrophobic to stretched/hydrophilic in response to the changes in pH. Before plasma treatment, linear current–voltage curves are observed at different pH (Figure 4B). After plasma treatment, remarkable ICR is found at neutral and basic pH (Figure 4C). Upon change of the pH from 5.8 to 2.8, a significant decrease in the transmembrane ionic current is observed. The open/close switching behavior is dominated

by the hydrophobic interaction inside nanopores.<sup>37</sup> This chemical modification strategy generates inhomogeneous surface charge distribution and structural asymmetry. Furthermore, two types of polymer brushes can be separately grafted onto the two ends of the nanopore (Figure 5D).<sup>38</sup> The resultant asymmetric nanofluidic system exhibits more functionality and responsiveness (see the following discussions).

**2.4. Transmembrane Wettability Differences.** The crystal structure of the KcsA potassium channel shows that both hydrophobic and hydrophilic segments are present along the ion conduction pathway, responsible for the high selectivity and rapid conduction rate.<sup>39</sup> These structural characteristics give us inspiration to build artificial analogues that efficiently transport water or ionic species by asymmetric wettability.

By using molecular dynamics simulations, we predicted a nanosized water pump and charge filter based on

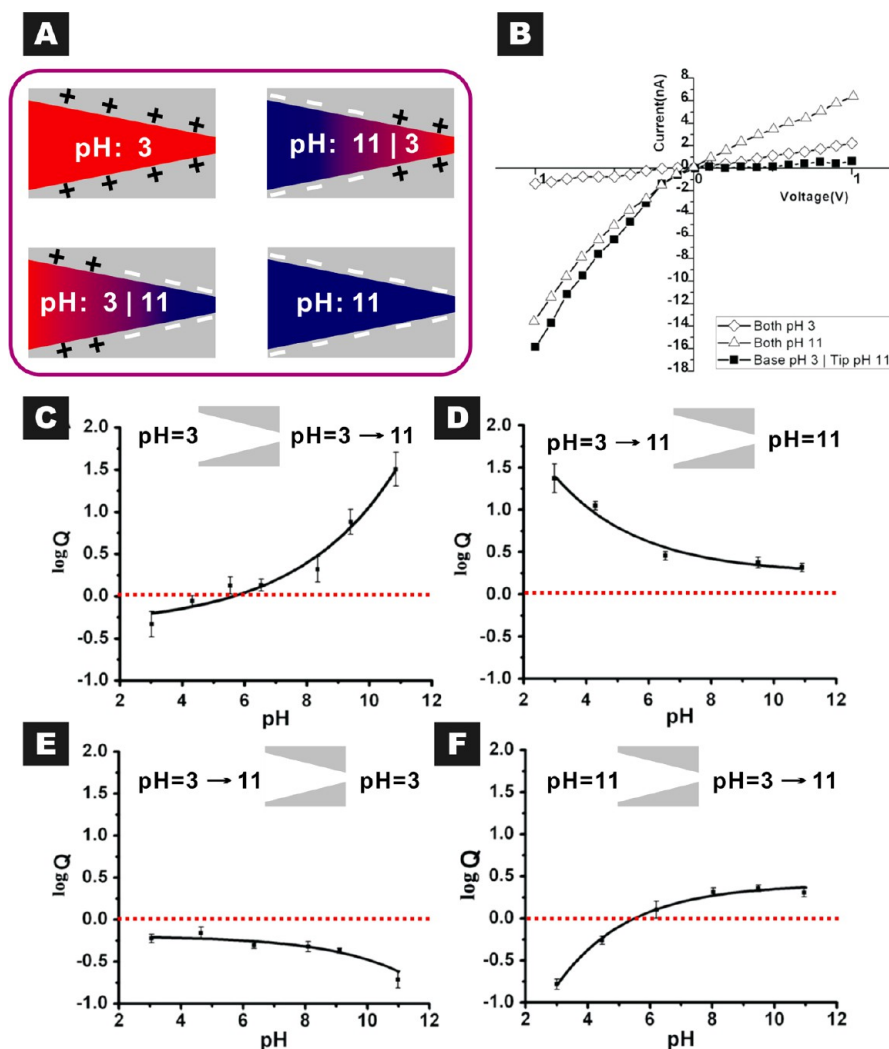


**FIGURE 6.** Ionic current rectification induced by pH gradient. (A, B) Compared with symmetric pH conditions (pH = 3 or 11 on both sides), a pH difference across the nanopore significantly enhances ionic rectification. (C–F) This hypothesis is further verified in four different conditions. “log  $Q$ ” represents the logarithm of the rectification ratio. The position of “zero” indicates a nonrectifying state.

asymmetrically modified single-wall carbon nanotubes (SWCNTs). Hydrophilic ( $-\text{COOH}$ ) and hydrophobic groups ( $-\text{CF}_3$ ) were separately modified on the two ends of the SWCNT (Figure 5A).<sup>40</sup> In pure water, by comparison of the water density ( $\rho(t)$ ) at the hydrophobic end (water II) and the hydrophilic end (water I) under equilibrium conditions, a distinguishable reduction in water density is found at the hydrophobic end, indicating that the water tends to transfer from the hydrophobic side to the hydrophilic side (Figure 5B). In a pristine SWCNT, the water density exhibits merely frequently overlap. The unidirectional water transport is achieved by an unbalanced chemical potential induced by the wettability difference (Figure 5C). In electrolyte solution, neither (6, 6) nor (8, 8) nanotubes allow the entrance of sodium or chloride ions due to high energy barriers at both ends. For the relatively wide (10, 10) and (12, 12) nanotubes,

ions are inclined to permeate to the side with low water density. This study suggests great possibilities for unidirectional water transport and desalination by tip-functionalized SWCNTs with asymmetric wettability.

Wettability gradient guided asymmetric ion transport has also been experimentally observed in chemically modified nanopores. We improve the plasma modification approach by separately modifying the hourglass-shaped nanopores with PNIPAAm and PAA on the two ends (Figure 5D).<sup>38</sup> Compared with the unmodified nanopores, the modified nanopores show distinct ionic rectifying properties (Figure 5E,F). Particularly, when there is wettability difference on the two sides (hydrophilic/hydrophobic), the nanopore exhibits the highest rectification ratio. A theoretical description is still required to clarify the underlying mechanism.

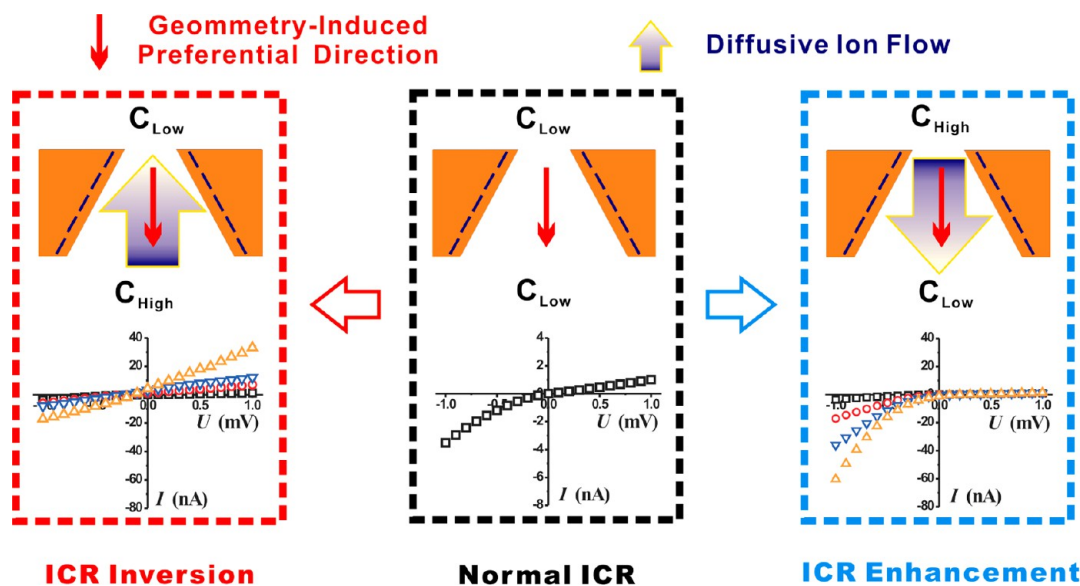


**FIGURE 7.** Concentration-gradient-dependent ionic current rectification in negatively charged conical nanopores. In symmetric electrolyte conditions, the cone-shaped geometry induces a preferential direction for ion transport from tip to base (normal ICR, middle). With a forwardly applied concentration gradient (from tip to base), the degree of ICR can be enhanced (right). With reversed concentration gradient (from base to tip), an unusual rectification inversion is observed (left). The ICR enhancement and inversion is attributed to the cooperation and competition between geometry-induced preferential ion transport (thin arrow) and the diffusive ion flow (thick arrow).

### 3. Asymmetric Ion Transport Controlled by Electrolyte Conditions

**3.1. pH Gradient across Nanopores.** A nanofluidic diode conducts ionic flow preferentially under one voltage bias and inhibits the ionic current under the opposite bias.<sup>41</sup> Pioneer works are theoretically predicted by Daiguji et al.<sup>42</sup> and experimentally investigated by Siwy et al.<sup>43</sup> and Karnik et al.<sup>28</sup> They adopt an asymmetric chemical modification by placing negative and positive charges onto separate parts of the channel wall analogous to a bipolar semiconductor diode. The rectification ratio can be tremendously enhanced by the heterogeneous surface charge distribution.

Taking track-etched nanopores in polymer membrane as an example, the surface charge results from the deprotonation of carboxyl groups, highly dependent on the local pH near the pore wall. Therefore, by simply adjusting the pH of the electrolyte solutions on the two sides of the nanopore (Figure 6A), we realize a highly efficient rectifying nanofluidic system without any chemical modification.<sup>44</sup> Compared with the two symmetric pH conditions (pH = 3 and 11 on both sides), the pH gradient across the nanopore results in pronounced ICR (Figure 6B). The nanopore is negatively charged at neutral or basic pH. The adsorption of protons at over acidic condition makes the local area positively charged. Thus, a bipolar nanopore forms in an asymmetric pH environment that is responsible for the enhanced rectification ratio (Figure 6C–F).

**3.2. Concentration-Gradient across Nanopores.** In living cells, the transmembrane concentration difference is fundamental to the membrane potential that regulates the ionic species inward and outward from the cell. Guo et al. report that a difference in ionic concentration induces rectified ion transport in homogeneous silica nanochannels.<sup>45</sup> In structurally asymmetric nanofluidic systems, the case is more interesting. Considering the inherent rectifying properties, both the direction and amplitude of ICR can be modulated by the ion concentration gradient.<sup>46</sup> For example, in charged conical nanopores, it is generally believed that the ICR is controlled by the nanopore geometry, electrolyte concentration, and pH.<sup>5</sup> In the presence of a concentration gradient, the rectification ratio is enhanced with the parallel diffusion current (from tip to base, Figure 7, right). When the concentration gradient is reversed (from base to tip, Figure 7, left), an unusual rectification inversion is observed. The concentration-gradient-dependent ICR enhancement and inversion is attributed to the cooperation and competition between geometry-induced asymmetric ion transport and the concentration-gradient-driven ionic flow.

The origin of this effect can be understood with an analytic model based on PNP equations. Upon a forward concentration gradient (Figure 7, right), the diffusive ion flow dominates the ion distribution inside the nanopore that brings in a considerable amount of counterions from the high-concentration bath. Under a negative potential, the electromigration of counterions is parallel to the diffusion current; therefore, the geometry-induced



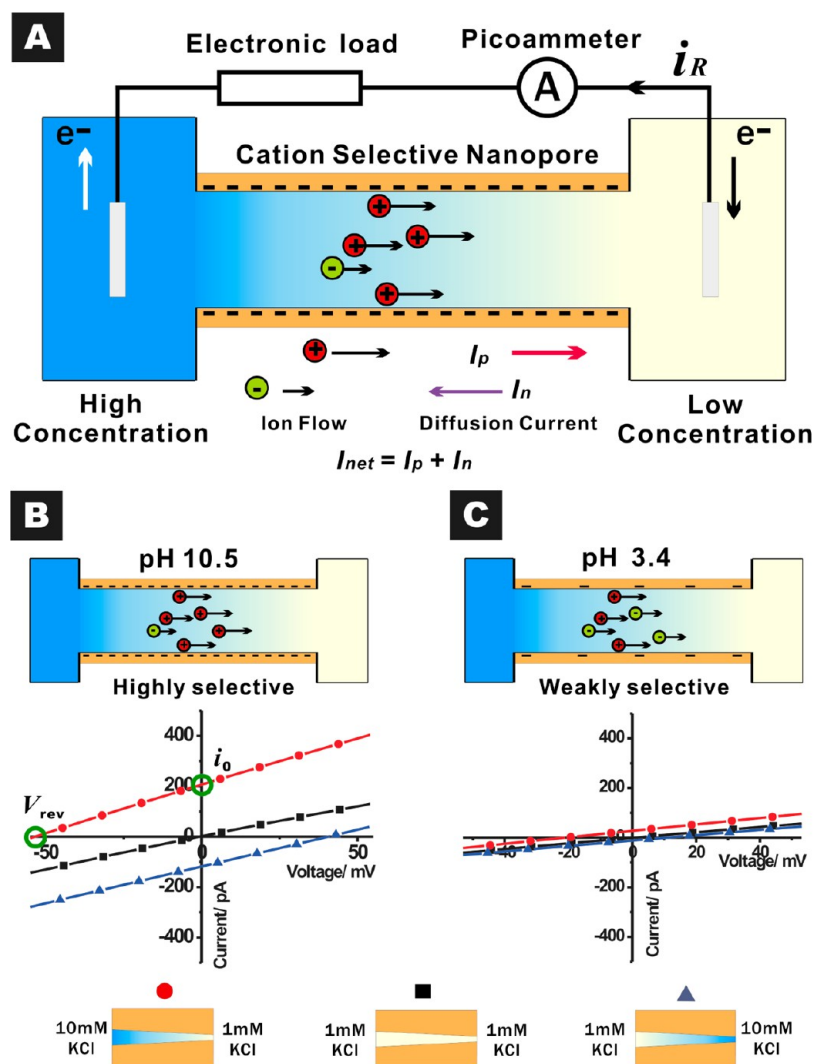


**FIGURE 8.** Generation of net diffusion current through cation-selective nanopores. (A) In negatively charged nanopores, cations are preferentially transported over anions. Driven by the concentration gradient, the ions diffuse spontaneously across the pore, generating net diffusion current. (B) In highly charged nanopores, the zero-volt current ( $i_0$ ) and reversal potential ( $V_{rev}$ ) can be clearly measured. (C) In weakly charged nanopores, the resulting  $i_0$  and  $V_{rev}$  is very limited.

ionic rectification is enhanced. Upon a reverse concentration gradient (Figure 7, left), however, the diffusion current is opposite to the geometry-induced preferential ion transport direction. In this case, at positive potential, the diffusive flow facilitates the counterion migration into the nanopore from the high-concentration bath, and at negative potentials, the diffusive flow prohibits the counterions from flowing into the nanopore leading to the rectification inversion.

**3.3. Generation of Net Diffusion Current.** The ion diffusion through a charged nanochannel generates net diffusion current (zero-volt current,  $i_0$ ).<sup>6</sup> When the salt concentrations on both sides are equal, no measurable  $i_0$  can be observed. In charged nanofluidic channels, counterions are preferentially transported over the co-ions, known as ion-selectivity (Figure 8A). Under the concentration difference, the spontaneous

ion diffusion generates a net ionic flow contributed by the counterions. In highly charged nanopores, the radial ion distribution proves that  $i_0$  stems from the separation of cations from anions within the EDL (Figure 8B).<sup>47</sup> If the surface-charge density is low, the degree of charge separation is greatly reduced, resulting in very limited  $i_0$  (Figure 8C). The generation of net diffusion current is very sensitive to the structure of EDL. Therefore, by finely tuning the surface charge properties, electrolyte condition, and nanopore geometry, the generation of net diffusion current can be well-controlled.

**3.4. Asymmetric Ion Mobility.** Toward a deep insight into the net diffusion current, we investigate the diffusive ionic flow in both cation- and anion-selective nanopores (Figure 9A) with three representative types of monovalent inorganic electrolytes: potassium chloride (KCl), sodium chloride (NaCl), and

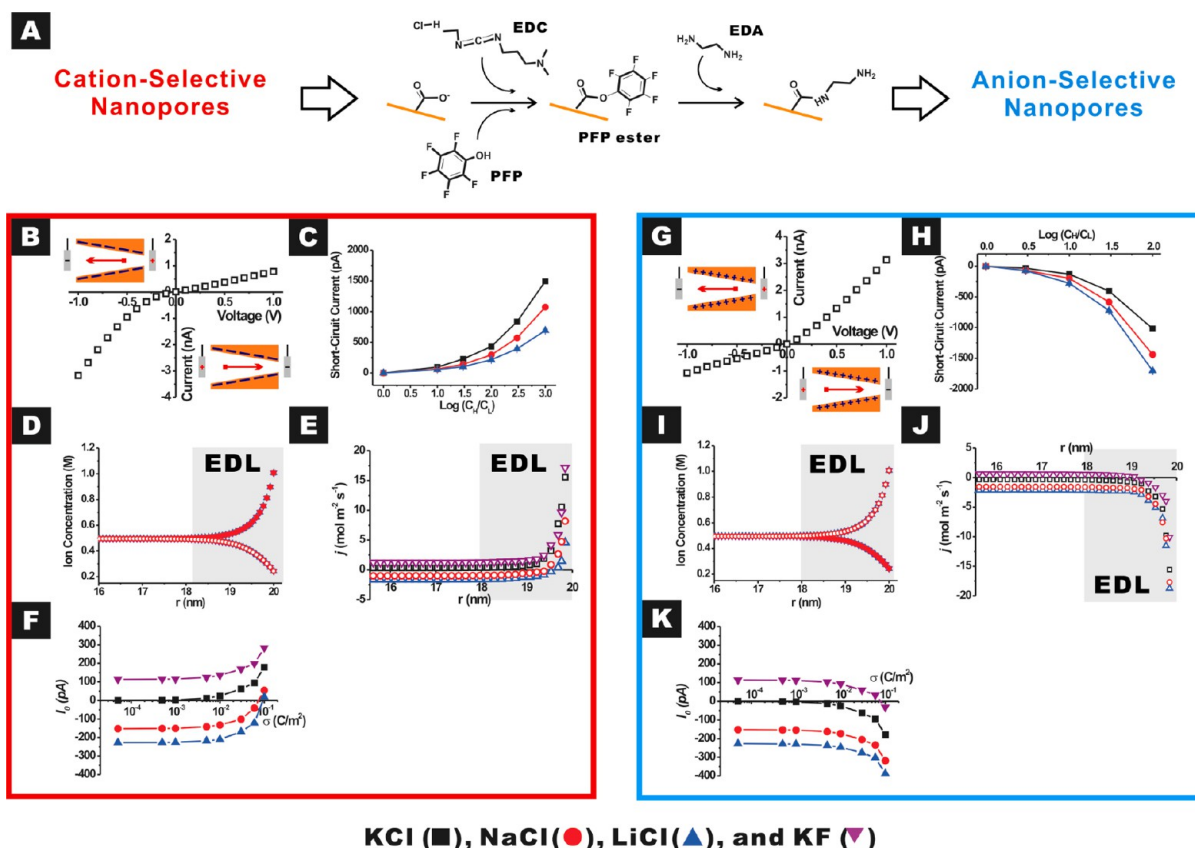


**FIGURE 9.** Diffusion current controlled by charge selectivity and asymmetric ion mobility. (A) Through a two-step chemical modification strategy, we fabricate both cation- (in red frame) and anion-selective nanopores (in blue frame). Four types of 1:1 inorganic salts, KCl, NaCl, LiCl, and KF, are studied. The diffusion current ( $i_0$ ) is very sensitive to the ionic composition of the electrolyte solution (C and H). Model calculations show that the radial ion distributions are identical for all four types of salt in either cation- (D) or anion-selective nanochannels (I). However, the resulting local current densities (E and J) and the total current (F and K) are quite different, due to the different ion mobility. The cooperation and competition between the asymmetric ion mobility and the charge selectivity play a crucial role.

lithium chloride (LiCl).<sup>48</sup> The net diffusion current is very sensitive to the ionic composition in both types of charge-selective nanopores (Figure 9C,H). In cation-selective nanopores, with the same type of anion ( $\text{Cl}^-$ ), the diffusion current increases with the cation mobility, while in anion-selective nanopores, this trend can be the opposite. From model calculations, two leading factors that dominate the charge separation in the diffusive nanofluidic system can be identified: (1) the charge selectivity of the nanopores and (2) the inherent asymmetric ion mobility between cations and anions (Figure 9D–F, I–K). The charge selectivity enhances the generation of net diffusion current if the inherent ion mobility of counterions is higher or approximately equal to that of the co-ions. Otherwise, it would reduce the magnitude of net diffusion current.

#### 4. Applications of Asymmetric Ion Transport Properties

In recent years, intensive efforts have been made in the application of the biomimetic nanofluidic devices with

asymmetric ion transport functions, including bioinspired energy conversion devices,<sup>4</sup> nanofluidic analytics,<sup>49</sup> seawater desalination,<sup>50</sup> etc. Herein, we highlight several examples in our group.

**4.1. Bioinspired Energy Conversion Systems.** Harnessing transmembrane ionic gradients into electricity by membrane-protein-regulated ion transportation is an intriguing process in many living cells.<sup>51</sup> Inspired by the electrogenic cell of the electric eel, we demonstrate a proof-of-concept nanofluidic reverse electro dialysis system (NREDS) that converts salinity gradient energy into electricity with ion-selective nanopores.<sup>47</sup> As illustrated in Figure 8, the diffusive ionic flow ( $i_0$ ) and the reversal potential ( $V_{\text{rev}}$ ) are considered as the short-circuit current ( $I_{\text{sc}}$ ) and the open-circuit voltage ( $U_{\text{oc}}$ ) of the nanofluidic power source. The maximum power output from a single-pore device approaches 26 pW. When parallelization with a pore density of  $10^8$ – $10^{10}$  cm<sup>-2</sup> is exploited, the estimated power density approaches 3–260 mW cm<sup>-2</sup>, which is 1–3 orders of magnitude higher than that using

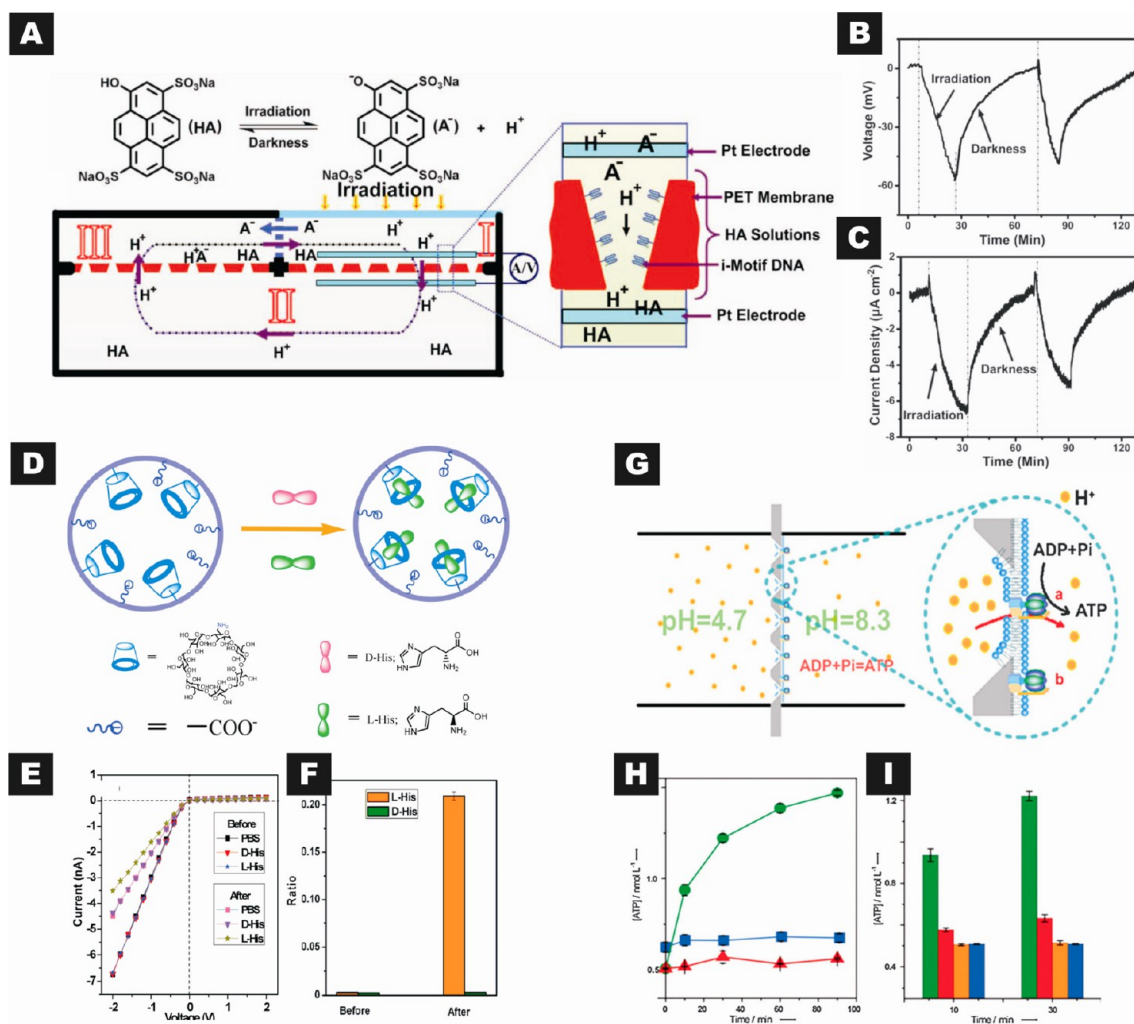


**FIGURE 10.** Some applications. (A–C) Scheme of the bioinspired photoelectric conversion system. It contains a three-compartment electrochemical cell that is separated by two sets of DNA-modified, proton-gated nanoporous membranes (between I and II, and II and III) and a piece of anion-exchange membrane (between I and III). HA is used as a light-driven proton pump to generate transmembrane proton motive force. The cyclic transport of HA through the three compartments forms a closed loop for the generation of photovoltage and photocurrent. (D–F) An enantioselective nanopore system is realized by covalently anchoring  $\beta$ -CD with the conical nanopores via carbodiimide coupling chemistry. The nanopore sensor shows highly selective recognition of histidine enantiomers (L-His) by detecting the rectified ionic current. (G–I)  $F_0F_1$ -ATPase is reconstituted in artificial nanoporous membranes. Under proton concentration gradient, ATP is synthesized on the F<sub>1</sub> side, in contrast to the two control groups (H). The activity of the enzyme gradually declined. The survival of the biohybrid device can maintain at least one day (I).

ion-exchange membranes ( $\sim 0.17 \text{ mW cm}^{-2}$ ). In addition, with a well-matched electrolyte type and nanopore charge selectivity, the power generation and the energy conversion efficiency of the NREDS can be further improved.<sup>48</sup>

In a further step toward nanofluidic energy conversion systems, we use photoacid molecules (8-hydroxypyrene-1,3,6-trisulfonate, HA) to generate the transmembrane proton concentration gradient upon light irradiation and harvest solar energy through proton-gated nanoporous membranes (Figure 10A).<sup>52</sup> The device is constructed in a three-compartment electrochemical cell. Two pieces of membranes containing DNA-modified, proton-gated nanopores are inserted between compartments I and II and between compartments II and III. An

anion-exchange membrane separates compartments I and III. The HA molecules function as a light-driven proton pump that release protons in compartment I upon UV irradiation and generate a transmembrane potential difference between compartments I and II. The cyclic transport of HA through the three compartments outputs continuous photovoltage and photocurrent to the external circuit (Figure 10B,C).

**4.2. Nanofluidic Sensing Devices.** Another important application is to build chemical analysis systems into the ion-channel-mimetic nanopores. When molecular analytes are present in the nanofluidic sensing system, they temporarily or permanently block the pathway for ion conduction, yielding characteristic changes in background current as

signatures for target identification.<sup>53</sup> For example, the nanofluidic diodes with highly nonlinear current–voltage responses can be further developed into biochemical sensors based on the local changes of surface charge properties.<sup>54</sup> The sensing events are monitored as the change in rectification ratio. Recently, we report a nanofluidic chiral analysis system based on the enantioselective recognition in  $\beta$ -cyclodextrin-modified single conical nanopores (Figure 10D).<sup>55</sup> The modified nanopore shows chiral-specific sensing of L-histidine by monitoring the rectified ionic current (Figure 10E,F).

**4.3. Biohybrid Nanofluidic Device for ATP Synthesis.** F-type ATP synthase ( $F_0F_1$ -ATPase) is a biological rotary motor that synthesizes ATP in living organisms. When proton flow comes from the intramembrane part ( $F_0$ ) driven by its concentration gradient, ATP synthesis is catalyzed on the extramembrane part ( $F_1$ ). We develop a biohybrid nanosystem, in which the  $F_0F_1$ -ATPase is reconstituted in liposome-coated solid-state nanopores (Figure 10G).<sup>56</sup> The activity of the biological motor is well preserved in the artificial system (Figure 10H,I). By application of a transmembrane proton concentration gradient ( $\text{pH} = 4.7/\text{pH} = 8.3$ ), ATP is synthesized on the  $F_1$  side. The ATP synthesis rate approaches 37 per second per enzyme molecule.

## 5. Conclusion and Outlook

This Account reviews recent progress on the control of asymmetric ion transport properties within biomimetic nanofluidic structures. Two asymmetric ion transport phenomena are discussed, the rectified ionic current and the net diffusion current. Several dominant factors for regulating the asymmetric ion transport properties are identified, which can be divided into two categories. One is to build the asymmetric factors directly into the nanofluidic structures, including nanopore geometry, surface charge distribution, different chemical composition, and traverse wettability differences. The other one is to construct different environmental conditions in the solution on the two sides of the nanofluidic channel, including the pH and concentration gradient across the nanochannel and the difference in ion mobility between cations and anions. These novel and well-controlled nanofluidic phenomena become the foundation for many applications, such as bioinspired energy conversion systems, nanofluidic sensing devices, and biohybrid nanodevices for in vitro biosynthesis.

Besides these mentioned factors, other crucial factors have also been reported in the literature, such as addition of surfactant,<sup>57</sup> electroosmotic flow,<sup>58</sup> and pressure-driven flow.<sup>59</sup> We believe that the upsurge in the investigation of asymmetric ion transport through synthetic nanochannels

has just started. More interesting phenomena and their underlying principles will be discovered. As to the application field, we will focus our research on the design of new bioinspired, smart, multiscale interfacial (BSMI) materials,<sup>60</sup> especially for the energy-oriented applications.

---

*This work is financially supported by the National Research Fund for Fundamental Key Projects (Grants 2011CB935700 and 2009CB930404), the National Natural Science Foundation of China (Grants 21103201, 11290163, 91127025, and 21121001), and the Key Research Program of the Chinese Academy of Sciences (Grant KJZD-EW-M01).*

---

### BIOGRAPHICAL INFORMATION

**Wei Guo** is currently an associate professor at the Institute of Chemistry, Chinese Academy of Sciences (ICCAS). He received a Ph.D. in physics from Peking University in 2009. Afterwards, he joined Prof. Lei Jiang's group in ICCAS. His scientific interests are focused on theoretical investigation of nanofluidic transport phenomena, fabrication of intelligent nanofluidic devices, and their applications on advanced energy conversion systems.

**Ye Tian** is currently an assistant professor at the Institute of Chemistry, Chinese Academy of Sciences (ICCAS). She received her B.S. degree from Northeast Normal University (Changchun, China) in 2006. Then she joined Prof. Lei Jiang's group as a Ph.D. candidate and received her Ph.D. in physical chemistry from ICCAS in 2011. Her scientific interests are focused on biomimetic smart single nanochannels.

**Lei Jiang** is a full professor at the Institute of Chemistry, Chinese Academy of Sciences (ICCAS), and dean of School of Chemistry and Environment, Beihang University. He received his Ph.D. from Jilin University in 1994. He then worked as a postdoctoral fellow in Prof. Akira Fujishima's group in Tokyo University. In 1996, he worked as a senior researcher in Kanagawa Academy of Sciences and Technology under Prof. Kazuhito Hashimoto. He joined ICCAS as part of the Hundred Talents Program in 1999. He was elected academician of Chinese Academy of Sciences in 2009 and the Academy of Sciences for the Developing World in 2012. His scientific interests are focused on bioinspired, smart, multiscale interfacial (BSMI) materials.

---

### FOOTNOTES

\*E-mail: jianglei@iccas.ac.cn.  
The authors declare no competing financial interest.

---

### REFERENCES

- Dekker, C. Solid-state nanopores. *Nat. Nanotechnol.* **2007**, *2*, 209–215.
- Hou, X.; Guo, W.; Jiang, L. Biomimetic smart nanopores and nanochannels. *Chem. Soc. Rev.* **2011**, *40*, 2385–2401.
- Pakhomov, A.; Bowman, A.; Ibey, B.; Andre, F.; Pakhomova, O.; Schoenbach, K. Lipid nanopores can form a stable, ion channel-like conduction pathway in cell membrane. *Biochem. Biophys. Res. Commun.* **2009**, *385*, 181–186.
- Sparreboom, W.; van den Berg, A.; Eijkel, J. C. T. Principles and applications of nanofluidic transport. *Nat. Nanotechnol.* **2009**, *4*, 713–720.

- 5 Siwy, Z. Ion-current rectification in nanopores and nanotubes with broken symmetry. *Adv. Funct. Mater.* **2006**, *16*, 735–746.
- 6 Siwy, Z.; Kosinska, I. D.; Fulinski, A.; Martin, C. R. Asymmetric diffusion through synthetic nanopores. *Phys. Rev. Lett.* **2005**, *94*, No. 048102.
- 7 Miles, B. N.; Ivanov, A. P.; Wilson, K. A.; Dogan, F.; Japrun, D.; Edell, J. B. Single molecule sensing with solid-state nanopores: Novel materials, methods, and applications. *Chem. Soc. Rev.* **2013**, *42*, 15–28.
- 8 Reiner, J. E.; Balijepalli, A.; Robertson, J. W. F.; Campbell, J.; Suehle, J.; Kasianowicz, J. J. Disease detection and management via single nanopore-based sensors. *Chem. Rev.* **2012**, *112*, 6431–6451.
- 9 Percec, V.; Dulcey, A. E.; Balagurusamy, V. S. K.; Miura, Y.; Smidrkal, J.; Peterca, M.; Nummelin, S.; Edlund, U.; Hudson, S. D.; Heiney, P. A.; Hu, D. A.; Magonov, S. N.; Vinogradov, S. A. Self-assembly of amphiphilic dendritic dipeptides into helical pores. *Nature* **2004**, *430*, 764–768.
- 10 Matile, S.; Jentzsch, A. V.; Montenegro, J.; Fin, A. Recent synthetic transport systems. *Chem. Soc. Rev.* **2011**, *40*, 2453–2474.
- 11 Barboiu, M. Artificial water channels. *Angew. Chem., Int. Ed.* **2012**, *51*, 11674–11676.
- 12 Hinds, B. Dramatic transport properties of carbon nanotube membranes for a robust protein channel mimetic platform. *Curr. Opin. Solid State Mater.* **2012**, *16*, 1–9.
- 13 Gouaux, E.; MacKinnon, R. Principles of selective ion transport in channels and pumps. *Science* **2005**, *310*, 1461–1465.
- 14 Hou, X.; Zhang, H.; Jiang, L. Building bio-inspired artificial functional nanochannels: From symmetric to asymmetric modification. *Angew. Chem., Int. Ed.* **2012**, *51*, 5296–5307.
- 15 Apel, P.; Korchev, Y.; Siwy, Z.; Spohr, R.; Yoshida, M. Diode-like single-ion track membrane prepared by electro-stopping. *Nucl. Instrum. Methods, Sect. B* **2001**, *184*, 337–346.
- 16 Liu, Q.; Wang, Y.; Guo, W.; Ji, H.; Xue, J.; Ouyang, Q. Asymmetric properties of ion transport in a charged conical nanopore. *Phys. Rev. E* **2007**, *75*, No. 051201.
- 17 Guo, W.; Xue, J.; Wang, L.; Wang, Y. Controllable etching of heavy ion tracks with organic solvent addition in etchant. *Nucl. Instrum. Methods, Sect. B* **2008**, *266*, 3095–3099.
- 18 Daiguji, H.; Yang, P.; Majumdar, A. Ion transport in nanofluidic channels. *Nano Lett.* **2003**, *4*, 137–142.
- 19 Pu, Q.; Yun, J.; Temkin, H.; Liu, S. Ion-enrichment and ion-depletion effect of nanochannel structures. *Nano Lett.* **2004**, *4*, 1099–1103.
- 20 Gao, J.; Guo, W.; Geng, H.; Hou, X.; Shuai, Z.; Jiang, L. Layer-by-layer removal of insulating few-layer mica flakes for asymmetric ultra-thin nanopore fabrication. *Nano Res.* **2012**, *5*, 99–108.
- 21 Wang, X.; Xue, J.; Wang, L.; Guo, W.; Zhang, W.; Wang, Y.; Liu, Q.; Ji, H.; Ouyang, Q. How the geometric configuration and the surface charge distribution influence the ionic current rectification in nanopores. *J. Phys. D* **2007**, *40*, 7077–7084.
- 22 Nishizawa, M.; Menon, V.; Martin, C. Metal nanotubule membranes with electrochemically switchable ion-transport selectivity. *Science* **1995**, *268*, 700–702.
- 23 Siwy, Z.; Heins, E.; Harrell, C.; Kohli, P.; Martin, C. Conical-nanotube ion-current rectifiers: The role of surface charge. *J. Am. Chem. Soc.* **2004**, *126*, 10850–10851.
- 24 Guo, W.; Xia, H.; Xia, F.; Hou, X.; Cao, L.; Wang, L.; Xue, J.; Zhang, G.; Song, Y.; Zhu, D.; Wang, Y.; Jiang, L. Current rectification in temperature-responsive single nanopores. *ChemPhysChem* **2010**, *11*, 859–864.
- 25 Hou, X.; Dong, H.; Zhu, D.; Jiang, L. Fabrication of stable single nanochannels with controllable ionic rectification. *Small* **2010**, *6*, 361–365.
- 26 Tian, Y.; Hou, X.; Jiang, L. Biomimetic ionic rectifier systems: Asymmetric modification of single nanochannels by ion sputtering technology. *J. Electroanal. Chem.* **2011**, *656*, 231–236.
- 27 Cheng, L.-J.; Guo, L. Ionic current rectification, breakdown, and switching in heterogeneous oxide nanofluidic devices. *ACS Nano* **2009**, *3*, 575–584.
- 28 Karnik, R.; Duan, C.; Castellino, K.; Daiguji, H.; Majumdar, A. Rectification of ionic current in a nanofluidic diode. *Nano Lett.* **2007**, *7*, 547–551.
- 29 Yameen, B.; Ali, M.; Neumann, R.; Ensinger, W.; Knoll, W.; Azzaroni, O. Single conical nanopores displaying pH-tunable rectifying characteristics. Manipulating ionic transport with zwitterionic polymer brushes. *J. Am. Chem. Soc.* **2009**, *131*, 2070–2071.
- 30 Zhou, Y.; Guo, W.; Cheng, J.; Liu, Y.; Li, J.; Jiang, L. High-temperature gating of solid-state nanopores with thermo-responsive macromolecular nanoactuators in ionic liquids. *Adv. Mater.* **2012**, *24*, 962–967.
- 31 Xia, F.; Guo, W.; Mao, Y.; Hou, X.; Xue, J.; Xia, H.; Wang, L.; Song, Y.; Ji, H.; Ouyang, Q.; Wang, Y.; Jiang, L. Gating of single synthetic nanopores by proton-driven DNA molecular motors. *J. Am. Chem. Soc.* **2008**, *130*, 8345–8350.
- 32 Hou, X.; Guo, W.; Xia, F.; Nie, F.-Q.; Dong, H.; Tian, Y.; Wen, L.; Wang, L.; Cao, L.; Yang, Y.; Xue, J.; Song, Y.; Wang, Y.; Liu, D.; Jiang, L. A biomimetic potassium responsive nanochannel: G-Quadruplex DNA conformational switching in a synthetic nanopore. *J. Am. Chem. Soc.* **2009**, *131*, 7800–7805.
- 33 Tian, Y.; Hou, X.; Wen, L.; Guo, W.; Song, Y.; Sun, H.; Wang, Y.; Jiang, L.; Zhu, D. A biomimetic zinc activated ion channel. *Chem. Commun.* **2010**, *46*, 1682–1684.
- 34 Guo, W.; Xia, H.; Cao, L.; Xia, F.; Wang, S.; Zhang, G.; Song, Y.; Wang, Y.; Jiang, L.; Zhu, D. Integrating ionic gate and rectifier within one solid-state nanopore via modification with dual-responsive copolymer brushes. *Adv. Funct. Mater.* **2010**, *20*, 3561–3567.
- 35 Jiang, Y.; Liu, N.; Guo, W.; Xia, F.; Jiang, L. Highly-efficient gating of solid-state nanochannels by DNA supersandwich structure containing ATP aptamers: A nanofluidic IMPLICATION logic device. *J. Am. Chem. Soc.* **2012**, *134*, 15395–15401.
- 36 Hou, X.; Liu, Y.; Dong, H.; Yang, F.; Li, L.; Jiang, L. A pH-gating ionic transport nanodevice: Asymmetric chemical modification of single nanochannels. *Adv. Mater.* **2010**, *22*, 2440–2443.
- 37 Powell, M.; Cleary, L.; Davenport, M.; Shea, K.; Siwy, Z. Electric-field-induced wetting and dewetting in single hydrophobic nanopores. *Nat. Nanotechnol.* **2011**, *6*, 798–802.
- 38 Hou, X.; Yang, F.; Li, L.; Song, Y.; Jiang, L.; Zhu, D. A biomimetic asymmetric responsive single nanochannel. *J. Am. Chem. Soc.* **2010**, *132*, 11736–11742.
- 39 Doyle, D.; Cabral, J.; Pfuetzner, R.; Kuo, A.; Gulbis, J.; Cohen, S.; Chait, B.; MacKinnon, R. The structure of the potassium channel: Molecular basis of K<sup>+</sup> conduction and selectivity. *Science* **1998**, *280*, 69–77.
- 40 Chen, Q.; Meng, L.; Li, Q.; Wang, D.; Guo, W.; Shuai, Z.; Jiang, L. Water transport and purification in nanochannels controlled by asymmetric wettability. *Small* **2011**, *7*, 2225–2231.
- 41 Cheng, L.-J.; Guo, L. Nanofluidic diodes. *Chem. Soc. Rev.* **2010**, *39*, 923–938.
- 42 Daiguji, H.; Oka, Y.; Shirono, K. Nanofluidic diode and bipolar transistor. *Nano Lett.* **2005**, *5*, 2274–2280.
- 43 Vlasiouk, I.; Siwy, Z. Nanofluidic diode. *Nano Lett.* **2007**, *7*, 552–556.
- 44 Wang, L.; Guo, W.; Xie, Y.; Wang, X.; Xue, J.; Wang, Y. Nanofluidic diode generated by pH gradient inside track-etched conical nanopore. *Radiat. Meas.* **2009**, *44*, 1119–1122.
- 45 Cheng, L.-J.; Guo, L. Rectified ion transport through concentration gradient in homogeneous silica nanochannels. *Nano Lett.* **2007**, *7*, 3165–3171.
- 46 Cao, L.; Guo, W.; Wang, Y.; Jiang, L. Concentration-gradient-dependent ion current rectification in charged conical nanopores. *Langmuir* **2012**, *28*, 2194–2199.
- 47 Guo, W.; Cao, L.; Xia, J.; Nie, F.; Ma, W.; Xue, J.; Song, Y.; Zhu, D.; Wang, Y.; Jiang, L. Energy harvesting with single-ion-selective nanopores: A concentration-gradient-driven nanofluidic power source. *Adv. Funct. Mater.* **2010**, *20*, 1339–1344.
- 48 Cao, L.; Guo, W.; Ma, W.; Wang, L.; Xia, F.; Wang, S.; Wang, Y.; Jiang, L.; Zhu, D. Towards understanding the nanofluidic reverse electrodiolysis system: Well matched charge selectivity and ionic composition. *Energy Environ. Sci.* **2011**, *4*, 2259–2266.
- 49 Piruska, A.; Gong, M.; Sweedler, J.; Bohn, P. Nanofluidics in chemical analysis. *Chem. Soc. Rev.* **2010**, *39*, 1060–1072.
- 50 Corry, B. Water and ion transport through functionalised carbon nanotubes: implications for desalination technology. *Energy Environ. Sci.* **2011**, *4*, 751–759.
- 51 Xu, J.; Sigworth, F.; LaVan, D. Synthetic protocells to mimic and test cell function. *Adv. Mater.* **2010**, *22*, 120–127.
- 52 Wen, L.; Hou, X.; Tian, Y.; Zhai, J.; Jiang, L. Bio-inspired photoelectric conversion based on smart-gating nanochannels. *Adv. Funct. Mater.* **2010**, *20*, 2636–2642.
- 53 Liu, N.; Jiang, Y.; Zhou, Y.; Xia, F.; Guo, W.; Jiang, L. Two-way nanopore sensing of sequence-specific oligonucleotides and small-molecule targets in complex matrices using integrated DNA supersandwich structures. *Angew. Chem., Int. Ed.* **2013**, *52*, 2007–2011.
- 54 Vlasiouk, I.; Kozel, T.; Siwy, Z. Biosensing with nanofluidic diodes. *J. Am. Chem. Soc.* **2009**, *131*, 8211–8220.
- 55 Han, C.; Hou, X.; Zhang, H.; Guo, W.; Li, H.; Jiang, L. Enantioselective recognition in biomimetic single artificial nanochannels. *J. Am. Chem. Soc.* **2011**, *133*, 7644–7647.
- 56 Dong, H.; Nie, R.; Hou, X.; Wang, P.; Yue, J.; Jiang, L. Assembly of F<sub>0</sub>F<sub>1</sub>-ATPase into solid state nanoporous membrane. *Chem. Commun.* **2011**, *47*, 3102–3104.
- 57 Wang, L.; Yan, Y.; Xie, Y.; Chen, L.; Xue, J.; Yan, S.; Wang, Y. A method to tune the ionic current rectification of track-etched nanopores by using surfactant. *Phys. Chem. Chem. Phys.* **2011**, *13*, 576–581.
- 58 Yusko, E.; An, R.; Mayer, M. Electroosmotic flow can generate ion current rectification in nano- and micropores. *ACS Nano* **2010**, *4*, 477–487.
- 59 Lan, W.; Holden, D.; White, H. Pressure-dependent ion current rectification in conical-shaped glass nanopores. *J. Am. Chem. Soc.* **2011**, *133*, 13300–13303.
- 60 Xia, F.; Jiang, L. Bio-inspired, smart, multiscale interfacial materials. *Adv. Mater.* **2008**, *20*, 2842–2858.